Int. J. Heat Mass Transfer. Vol. 22, pp. 679–689

0017-9310/79/0501-0679 $02.00/0

A REYNOLDS ANALOGY SOLUTION FOR THE HEAT TRANSFER CHARACTERISTICS OF COMBINED TAYLOR VORTEX AND AXIAL FLOWS

D. A. SIMMERS
U.K.A.E.A., Risley, U.K.
and
J. E. R. CONEY
Department of Mechanical Engineering, University of Leeds, Leeds LS2 9JT, U.K.

(*Received* 16 *October* 1978)

Abstract—A solution, similar to the Reynolds analogy solution for heat transfer and momentum, was developed for heat transfer between the outer surface of an annulus, formed by a stationary outer cylinder and a rotatable inner cylinder, and the fluid in the annulus; within the fluid, Taylor vortices and an imposed axial flow exist. To facilitate the solution, a three-part velocity profile was assumed, consisting of a laminar sub-layer adjacent to the annulus outer surface, a buffer layer and a core region of constant velocity in the central part of the annular gap. Expressions were obtained for the thicknesses of and temperature drops across the laminar sub-layer and buffer layer. These were used to give Nusselt numbers, which were compared with those obtained experimentally.

NOMENCLATURE

A, a constant $[1+N^2+(1-N^2)/\ln N]/[2+(1-N^2)/\ln N]$;
B, a dimensionless function;
c, a constant;
C_p, specific heat of fluid at constant pressure;
d, annular gap width, (R_2-R_1);
f, friction factor (various suffices);
f_1, friction factor for Poiseuille flow;
f_2, friction factor for Couette flow;
f_3, friction factor for combined Taylor vortex and axial flows;
h, heat-transfer coefficient;
k, thermal conductivity of the fluid;
N, annulus radius ratio (R_1/R_2);
Nu, Nusselt number $(2hd/k)$;
Pr, Prandtl number $(C_p v\rho/k)$;
$\dot{q}$, rate of heat transfer per unit area;
R, general radial coordinate;
R_1, radius of inner annular surface;
R_2, radius of outer annular surface;
Re_a, axial Reynolds number $(2u_{av}d/v)$;
T, temperature;
ΔT, temperature difference;
T_{av}, average temperature at a given section;
T_w, wall temperature;
Ta, Taylor number, $\Omega_1^2 R_1 d^3/v^2$ (narrow gap case, $N = 0.955$), $\dfrac{2\Omega_1^2 R_1^2 d^3}{v^2(R_1+R_2)}$ (wide gap case, $N = 0.8$);
Ta_c, critical value of Taylor number;
u_{av}, average axial velocity at a given section;
v, tangential velocity component;
v_r, tangential velocity of the rotor;
v^+, frictional tangential velocity, $v/(\tau_w/\rho)^{1/2}$;
y, distance from the heated surface;
y^+, frictional distance from the heated surface, $\dfrac{y(\tau_w/\rho)^{1/2}}{v}$.

Greek symbols

ε_H, eddy diffusivity for heat;
ε_M, eddy diffusivity for momentum;
v, kinematic viscosity of fluid;
ρ, density of fluid;
τ_{w1}, wall shear stress due to Poiseuille flow;
τ_{w2}, wall shear stress due to Couette flow;
τ_{w3}, wall shear stress due to combined Taylor vortex and axial flow;
Ω_1, angular velocity of the inner annular surface.

INTRODUCTION

FOR THE case of zero axial flow of a fluid in an annulus, the outer wall of which is heated and the inner rotatable, heat transfer between the heated wall and the fluid relies only on the tangential velocity component, since the axial and radial components consist merely of fluctuations about zero velocity. Thus, in the analogy solution of Bjorklund and Kays [1], the assumed velocity profiles were based on the results of Pai [2], which indicated that the tangential velocity profile consisted of regions of large velocity

gradient, close to the annular boundaries, surrounding a central region over which a constant velocity, equal to half of the inner cylinder peripheral velocity, prevailed. Hence, according to the analogy between heat and momentum transfer, the radial temperature distribution assumed in [1] consisted of a central region of constant temperature, bounded by regions of high temperature gradient, close to the annular boundaries. However, experimental radial temperature profiles from [1] indicated that a small temperature gradient existed across the central portion of the gap. Despite the neglect of this temperature gradient, the results of this analogy solution were in reasonable accord with the experimental heat transfer measurements. Because of the authors' interest in heat transfer in an annulus formed by a heated outer cylinder and an inner adiabatic rotating cylinder, with axial fluid flow, a similar analogy has been developed to take into account the effects of an imposed axial flow through the annulus.

For the case of an imposed axial flow, both the tangential and axial velocity components have an associated mean velocity, whilst only the radial component consists of fluctuations about zero velocity. Thus, for this case, the choice of the velocity profile to be used in the analogy is less clear, since both axial and tangential velocity components could be important in the transfer of heat. However, shear stress investigations and velocity profile studies [3] indicated that the Taylor vortices, once extablished in the annulus, act as though the axial flow were not present; the only noticeable effect of the imposed axial flow is the delay of vortex onset. In addition, velocity measurements [3] demonstrated the dominance of the tangential velocity component in the Taylor vortex regime of flow, and, thus, it may be assumed that, in this regime, the mechanisms of heat transfer rely heavily on the tangential velocity profile. Hence, the assumed velocity profile, included in the present analogy, is based on the tangential velocity data from [3], although, as will be shown later, the effects of the imposed axial flow are implicit in the formulation of the analogy.

The tangential velocity data [3] indicated that the velocity data of Pai [2] was erroneous; the velocity across the centre of the gap was not found to be constant, a small velocity gradient being observed, in accord with [4]. According to momentum transport theory, there should likewise be a small temperature gradient across this same central portion of the gap, as was observed in [1]. It was thought desirable to include the effects of this temperature gradient in the present analogy solution, for that solution to truly represent the actual flow conditions prevailing.

However, Taylor [4] and Flower [5] indicated that momentum transport theory is only applicable in the vicinity of the annular boundaries. Taylor, in particular, showed that the radial temperature distributions derived from his velocity data by the momentum transport theory were in disagreement with those actually obtained across the central portion of the gap. This finding is also implicit in the theoretical model of Batchelor [6] and stems from the consideration that, in Taylor vortex flow, the vortices effecting heat transfer are not small compared with the gap width. In addition, the vortices lack a net component of motion perpendicular to the heat transfer surface. Consequently, the concept of eddy diffusivity, in the classical sense, is inappropriate in this case; instead, the processes of convection are associated with the internal motions of the individual large vortices. This mechanism of heat transfer may be referred to as vorticity transport theory, which differs from the more familiar momentum transport theory in that there is no general correspondence between the heat transferred and the local temperature gradient.

Thus, for the present case, the effects of the predicted temperature gradient across the centre of the gap cannot be included in the formulation of the analogy between heat and momentum transfer. Neglect of this temperature gradient in [1] did not lead to serious differences between the predicted and measured values of Nusselt number, and this fact, in conjunction with the improved velocity data available to the authors, suggests that the present analogy should yield results in reasonable agreement with experimental measurements.

VELOCITY PROFILES ASSUMED FOR THE ANALOGY SOLUTION

The only velocity information required for the present analogy relates to the boundary layers close to the outer annular surface (heat-transfer surface) where the heat and momentum transfer analogy is applicable. Such information is not required at the inner wall, since it is assumed that no heat transfer occurs there. Also, in the central portion of the gap, since the analogy between heat and momentum transfer is not applicable, such information cannot impart knowledge of the temperature profiles obtaining.

The velocity distribution close to the outer annular wall was assumed to be similar to that obtained in the boundary layers of turbulent duct flow, modified to fit phenomena observed in the present situation. A three part velocity profile was assumed, consisting of a laminar sublayer adjacent to the outer annular surface, a buffer layer and finally a core region of constant velocity spanning the central portion of the gap. The assumed velocity distributions obtaining in the boundary layers cannot be compared with the velocity data of [3], since it was impossible to take accurate velocity measurements in the region of low velocity close to the outer wall.

FRICTION FACTORS IN COMBINED TAYLOR VORTEX AND AXIAL FLOW

The present analogy solution requires the definition of three friction factors, applicable to Poiseuille flow (pure axial flow), Couette flow

(laminar rotational flow) and to combined Taylor vortex and axial flows, necessary for the determination of the laminar sublayer and buffer layer thicknesses.

(a) *Friction factor for Poiseuille flow*, f_1

The shear stress of Poiseuille flow may be shown to be:

$$\tau_{w1} = \frac{\eta^2 Re_a}{A\rho d R_2}. \tag{1}$$

A friction factor for laminar, fully developed axial flow may be defined as:

$$f_1 = \frac{\tau_{w1}}{\rho u_{at}^2/2}. \tag{2}$$

From (1) and (2)

$$f_1 = \frac{8(1-N)}{ARe_a}. \tag{3}$$

(b) *Friction factor for Couette flow*, f_2

For the narrow gap case (i.e. $N \to 1$), the straight line velocity profile of Couette flow results in a constant velocity gradient across the gap equal to v_r/d). Thus, for this flow, a friction factor can be defined as:

$$f_2 = \frac{\tau_{w2}}{\rho v_r^2/2} = \frac{\eta v_r/d}{\rho v_r^2/2}. \tag{4}$$

Noting that,

$$Ta = \frac{v_r^2 d^3}{\nu^2 R_1} \text{ (narrow gap assumption)},$$

(4) becomes

$$f_2 = 2\left[\frac{1-N}{NTa}\right]^{1/2}. \tag{5}$$

(c) *Friction factor for combined Taylor vortex and axial flows*, f_3

Let
$$f_3 = \frac{\tau_{w3}}{\rho v_r^2/2}. \tag{6}$$

Since the velocity distribution for this flow is not known, and cannot be easily formulated mathematically, there exists no simple equation for τ_{w3}, such as those for Poiseuille and Couette flows. However, in [3] it was shown experimentally that:

$$\frac{\tau_{w3}}{\tau_{w1}} = \left[\frac{Ta}{Ta_c}\right]^{0.735}. \tag{7}$$

Now from equations (2) and (6), it may be shown that:

$$f_3 = \frac{2(1-N)^2}{AN}\frac{Re_a}{Ta}\frac{\tau_{w3}}{\tau_{w1}}. \tag{8}$$

THICKNESSES OF LAMINAR SUBLAYER AND BUFFER LAYER

(a) *Laminar sublayer*

The velocity distribution in the laminar sublayer was assumed to be of the form:

$$v^+ = y^+, \tag{9}$$

where v^+ is the tangential friction velocity obtaining at y^+, the non-dimensional radial distance from the heated surface.

The velocity data of [3] and the results of El-Shaarawi [7] indicate that, in the laminar, pre-vortex regime, the axial and tengential velocity profiles are independent, each attaining the fully developed profile identical to that for pure axial and pure rotational flows respectively. Thus, the point of critical stability is assumed to occur when the tangential laminar sublayers, growing with increase in Ta for a given Re_a on the annular boundaries, occupy the entire gap. El-Shaarawi [7] showed that, in a finite annular gap, the boundary layers growing on the flow boundaries were not symmetrical, but that, for decreasing gap width (i.e. $N \to 1$), the boundary-layer thicknesses approached equality. Thus, for Couette flow, and assuming that $N \to 1$, the sublayers will meet at the mid-gap point, at which position the tangential velocity is equal to half the rotor velocity.

It is well known that Taylor vortices first appear near to the inner rotating wall and this is usually taken as the critical condition. After this initial onset, a further increase in the Taylor number causes the vortices to expand towards the outer stationary wall. Also the authors have shown [8], by shear stress measurements taken at this wall, that, for the case of an imposed axial laminar flow, the effect of vortex flow (*viz.* a sharp increase in shear stress) is not noted until a Taylor number, much higher than the accepted critical value for the prevailing conditions, is reached. Hence, criticality, for the purpose of the present study, was not defined by critical vortex onset but by the close approach of the vortices to the outer wall, when they begin to affect both heat transfer and shear stress. It must also be assumed that the vortices have a negligible on the Couette velocity profile until the critical Taylor number, obtained from shear stress measurements, has been obtained. Under these conditions of criticality, equation (9) becomes:

$$y_1^+ = \frac{v_r/2}{(\tau_{w2}/\rho)^{1/2}} \tag{10}$$

where y_1^+ represents the non-dimensional distance from the heated surface to the edge of the laminar sublayer. Under these postulated conditions, Couette flow was assumed to prevail, and, therefore, τ_{w2} was used. Now, from equations (4), (5) and (10), it may be shown that:

$$y_1^+ = \frac{1}{2}\left(\frac{NTa_c}{1-N}\right)^{1/4}. \tag{11}$$

(b) *Buffer layer*

For the buffer layer, a Karman–Nikuradse type of velocity profile was assumed, of the form:

$$v^+ = c\left[1 + \ln\left(\frac{v^+}{c}\right)\right]. \tag{12}$$

The value of A, a constant, for the present case was chosen to maintain continuity of slope at the junction of the laminar sublayer and the buffer layer. From equations (11) and (9), it can be seen that:

$$v_1^+ = y_1^+ = \frac{1}{2}\left(\frac{NTa_c}{1-N}\right)^{1/4}$$

and continuity of slope is maintained if

$$c = \frac{1}{2}\left(\frac{NTa_c}{1-N}\right)^{1/4}.$$

Therefore, the assumed velocity profile becomes:

$$v^+ = \frac{1}{2}\left(\frac{NTa_c}{1-N}\right)^{1/4} \left\{1 + \ln\left[\frac{y^+}{\frac{1}{2}\left(\frac{NTa_c}{1-N}\right)^{1/4}}\right]\right\}, \quad (13)$$

which can be rewritten as:

$$y^+ = \frac{1}{2}\left(\frac{NTa_c}{1-N}\right)^{1/4} \exp\left[2\left(\frac{1-N}{NTa_c}\right)^{1/4} v^+ - 1\right]. \quad (14)$$

From the velocity data of [3], the tangential velocity component of Taylor vortex flow was shown to be characterised by a flattened central portion, bounded by regions of high velocity gradient, close to the annular boundaries. Although the velocity at the outer edge of this flattened region did not bear a direct relationship to the rotor velocity, it was found to correspond approximately to $v = v_r/3$ at the higher Taylor numbers investigated. Bjorklund and Kays [1] assumed that the velocity at this point, in the case of zero axial flow, corresponded to $v = v_r/2$, but the present results indicate that this assumption did not apply with imposed axial flow. Hence, assuming that the velocity at the edge of the buffer layer is equal to $v_r/3$, the frictional tangential velocity there becomes:

$$v_b^+ = \frac{v_r/3}{(\tau_{w3}/\rho)^{1/2}}. \quad (15)$$

τ_{w3}, the shear stress due to combined Taylor vortex and axial flows, is used in equation (14), as the buffer layer only exists under such flow conditions; it does not exist in the laminar pre-vortex regime.

From equations (6), (14) and (15), it may be shown that:

$$y_b^+ = \frac{1}{2}\left[\frac{NTa_c}{1-N}\right]^{1/4} \exp\left\{\frac{2}{3}\left(\frac{1-N}{NTa_c}\right)^{1/4}\left(\frac{2}{f_3}\right)^{1/2} - 1\right\}, \quad (16)$$

where y_b^+ is the non-dimensional distance from the heated surface to the edge of the buffer layer.

TEMPERATURE DROPS ACROSS THE LAMINAR SUBLAYER AND THE BUFFER LAYER

(a) *Assumptions of the analogy solution*

A number of simplifying assumptions are required to allow solution of the present analogy. Some of these stem from the usual simplifications associated with any Reynolds analogy solution, whilst others result from the particular flow being investigated. These assumptions are as follows:

(i) The laminar sublayer and buffer layer were considered sufficiently thin such that the shear stress and heat flux through them could be considered constant at τ_w and $\dot{q}$ respectively.

(ii) The radius ratio was assumed to approach unity (i.e. narrow gape case) to allow the use of a simplified shear stress equation:

$$\tau_w = \rho(\nu + \varepsilon_M)\frac{dv}{dy}. \quad (17)$$

For the finite gap case, dv/dy might more properly have been replaced by $(dv/dy - v/y)$ for transport of moment of momentum; however, v/y becomes small relative to dv/dy with decreasing gap width, and equation (17) adequately describes the narrow gap shear stress relationship.

(iii) The eddy diffusivities for heat and momentum were assumed to be equal.

(iv) The Prandtl number is assumed to equal unity. For air, this condition is closely approximated.

(v) Fully developed flow conditions prevail.

(vi) Temperature drops only occur across the laminar sublayer and buffer layer at the outer annular surface; the remainder of the annular gap is assumed to be a region of constant temperature.

On the basis of these assumptions, the temperature drops across the sublayers were assessed as follows.

(b) *Laminar sublayer*

Heat transfer occurs by conduction in this sublayer.

$$\therefore \quad \dot{q} = k\frac{dT}{dy} \quad (18)$$

$$\text{or} \quad \dot{q} = \frac{C_p \rho \nu}{Pr}\frac{dT}{dy}. \quad (19)$$

Integrating over the laminar sublayer yields:

$$\Delta T_1 = \frac{\dot{q} Pr}{C_p \rho \nu} y_1. \quad (20)$$

Therefore, from equation (11),

$$\Delta T_1 = \frac{\dot{q} Pr}{C_p \rho}\frac{\rho}{(\tau_w)^{1/2}}\frac{1}{2}\left(\frac{NTa_c}{1-N}\right)^{1/4}. \quad (21)$$

(c) *Buffer layer*

The buffer layer is considered to be a turbulent region, and thus the shear stress dependency becomes:

$$\tau_b = (\nu + \varepsilon_M)\rho\frac{dv}{dy} \quad (22)$$

where τ_b is the shear stress obtaining across the buffer layer. Also,

$$\frac{dy}{dv} = \frac{\rho \nu}{\tau_w}\frac{dy^+}{dv^+} \quad (23)$$

and differentiation of the assumed buffer layer velocity profile, equation (13), yields:

$$\frac{dv^+}{dy^+} = \frac{1}{2}\left[\frac{NTa_c}{1-N}\right]^{1/4}\frac{1}{y^+}. \quad (24)$$

Combining (22), (23) and (24) gives:

$$\varepsilon_M = \frac{\tau_b}{\rho}\frac{\rho\nu}{\tau_w}2y^+\left[\frac{1-N}{NTa_c}\right]^{1/4} - \nu. \quad (25)$$

From assumption (i), $\tau_b = \tau_w$ and hence equation (25) becomes:

$$\varepsilon_M = 2\nu y^+\left[\frac{1-N}{NTa_c}\right]^{1/4} - \nu. \quad (26)$$

In the buffer layer, heat transfer occurs by forced convection due to the turbulent nature of that region, and so

$$\dot{q}_b = \rho C_p(\varepsilon_H + k/\rho C_p)\frac{dT}{dy}, \quad (27)$$

where $\dot{q}_b$ is the heat-transfer rate, per unit area of heated surface, across the buffer layer. Thus, invoking assumption (i), i.e. $\dot{q}_b = \dot{q}$, and integrating over the width of the buffer layer, yields:

$$\int_{T_1}^{T_b} dT = \frac{\dot{q}}{\rho C_p}\int_{y_1}^{y_b}\frac{dy}{(\nu/Pr + \varepsilon_H)}. \quad (28)$$

From assumption (iii), $\varepsilon_M = \varepsilon_H$, and substituting for ε_M from equation (26), the temperature drop across the buffer layer becomes:

$$\Delta T_b = \frac{\dot{q}}{\rho C_p}\left(\frac{\rho}{\tau_w}\right)^{1/2}\int_{y_1^+}^{y_b^+} \times \frac{dy^+}{1/Pr + 2y^+\left(\frac{1-N}{NTa_c}\right)^{1/4}} - 1. \quad (29)$$

Integrating the right hand side of equation (29) and substituting in the limits of y_b^+ and y_1^+, as given by equations (11) and (16), gives:

$$\Delta T_b = \frac{\dot{q}}{\rho C_p}\left(\frac{\rho}{\tau_w}\right)^{1/2} \times \frac{1}{2}\left(\frac{NTa_c}{1-N}\right)^{1/4}\left(\ln\left\{1 + Pr\exp\left[\frac{2}{3}\left(\frac{1-N}{NTa_c}\right)^{1/4} \times \left(\frac{2}{f_3}\right)^{1/2} - 1\right] - Pr\right\}\right). \quad (30)$$

Hence the total temperature drop across the laminar sublayer and buffer layer, which according to assumption (vi) is the only temperature drop occurring across the gap width, becomes from equations (21) and (30):

$$\Delta T = \Delta T_1 + \Delta T_b = \frac{\dot{q}}{\rho C_p}\left(\frac{\rho}{\tau_w}\right)^{1/2} \times \frac{1}{2}\left(\frac{NTa_c}{1-N}\right)^{1/4}\left(Pr + \ln\left\{1 + Pr\exp\left[\left(\frac{1-N}{NTa_c}\right)^{1/4} \times \frac{2}{3}\left(\frac{2}{f_3}\right)^{1/2} - 1\right] - Pr\right\}\right). \quad (31)$$

Let

$$B = Pr + \ln\left\{1 + Pr\exp\left[\left(\frac{1-N}{NTa_c}\right)^{1/4} \times \frac{2}{3}\left(\frac{2}{f_3}\right)^{1/2} - 1\right] - Pr\right\} \quad (32)$$

$$\therefore \Delta T = \frac{\dot{q}}{\rho C_p}\left(\frac{\rho}{\tau_w}\right)^{1/2}\frac{1}{2}\left[\frac{NTa_c}{1-N}\right]^{1/4}B. \quad (33)$$

DERIVED NUSSELT NUMBER RELATIONSHIP

It may be shown by dimensional analysis that for combined Taylor vortex and axial flows

$$Nu = \phi(Re_a, Ta, Pr).$$

The Nusselt number is defined as

$$Nu = \frac{2hd}{k}. \quad (34)$$

Hence, from (6), (7), (8) and (34), and noting that $\tau_{w3} = \tau_3$, it may be shown that:

$$Nu = \frac{4\,Pr\,Re_a^{0.5}\,Ta^{0.3675}}{B\left(\frac{A}{1-N}\right)^{1/2}\left(\frac{N}{1-N}\right)^{1/4}Ta_c^{0.6175}}. \quad (35)$$

Also from (32),

$$B = Pr + \ln\left\{1 + Pr \times \exp\left[\frac{2}{3}\left(\frac{1-N}{N}\right)^{1/4}\left(\frac{NA}{(1-N)^2}\right)^{1/2} Re_a^{-0.5}\,Ta^{0.1325}\,Ta_c^{0.1175} - 1\right] - Pr\right\}. \quad (36)$$

Equations (35) and (36) represent the correlation equation for the heat transfer characteristics of combined Taylor vortex and laminar axial flows, as derived from the analogy between heat and momentum transfer. The equations, as presented, are applicable to the secondary regime of flow, referred to in [8]. However, the results of [8] also indicated that a tertiary regime of flow existed at the lower axial Reynolds numbers investigated, which was characterised by a further increase in slope of the shear stress vs Taylor number graph. For this regime, the results were still correlated by equation (7), but the exponent, n, of this equation was altered to 1.022 for $Re_a = 300$ and 0.927 for $Re_a = 400$. Hence equations (35) and (36) may also be used to determine the heat-transfer characteristics of the tertiary regime, provided that the exponents of Ta and Ta_c are altered accordingly.

RESULTS OF THE ANALOGY SOLUTION

Bjorklund and Kays [1] derived a similar, although simpler, equation to that presented in equations (35) and (36). For a Taylor number in excess of 8000, the Nusselt number was found to depend on $Ta^{0.380}$, compared with $Ta^{0.3675}$ (equation 35). Thus, despite the fact that different velocity and shear stress data were used in the two analogy solutions, and that one is applicable to zero axial flow whilst the other includes the effects of an

imposed axial flow, both solutions yield a similar functional dependency of Nusselt number on Taylor number. This similarity stems mainly from the agreement of the shear stress study of [8] with the results of Taylor [4], which were used by Bjorklund and Kays [1].

The results of the analogy solution for $N = 0.955$ and 0.8 were calculated from equations (35) and (36), using the values of Ta_c as given in Table 1. These results are presented in Figs. 1(a) and (b). The range of variables used was identical with that of [3], i.e. $300 \leqslant Re_a \leqslant 1600$, $Ta_c \leqslant Ta \leqslant 2 \times 10^6$.

From Figs. 1(a) and (b), it can be seen that in the primary regime, where vortices are absent or are present but unimportant, a constant value of Nusselt number prevails. Evaluation of equations (35) and (36) at criticality (i.e. $Ta = Ta_c$) gave, for each radius ratio, a similar value of calculated Nusselt number, regardless of the superimposed axial flow. These values of Nusselt number prevailing at critical conditions were averaged, and this mean value was plotted in Fig. 1(a) and (b), where it was assumed to apply to the whole of the primary regime. The average values of Nusselt number were determined

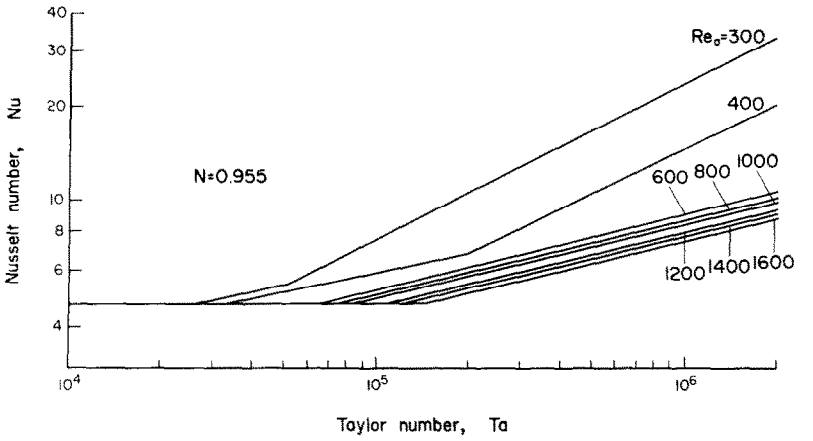

(a)

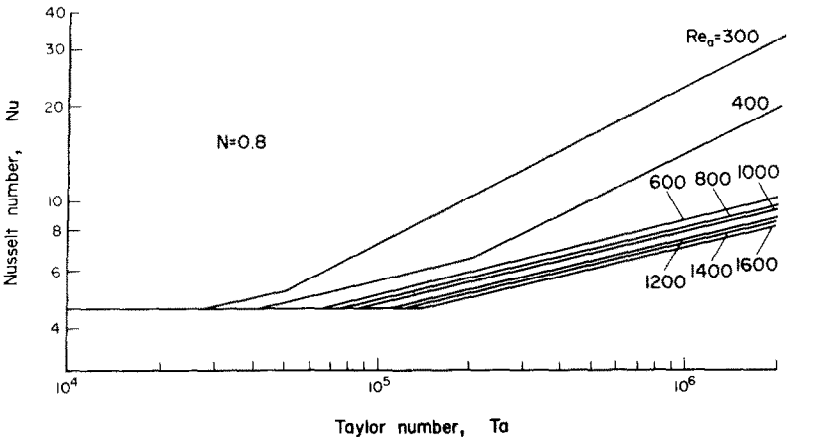

(b)

FIG. 1. Results of Reynolds analogy solution.

Table 1. Variation of critical Taylor number with axial Reynolds number

Re_a	Ta_c
300	28,000
400	41,000
600	62,000
800	78,000
1000	84,000
1200	110,000
1400	119,000
1600	142,000

as 4.902 for $N = 0.955$ and 4.783 for $N = 0.8$, which may be compared with the theoretical values due to El-Shaarawi [7] of 4.823 and 4.697 for $N = 0.955$ and 0.8 respectively. In [3] it was shown that, according to the analogy between heat and momentum transfer, the shear stress results obtained for the primary regime predicted a constant value of Nusselt number throughout that regime. Although the present analogy solution does not apply to the primary regime, at the limiting conditions of $Ta = Ta_c$ (the demarcation between the primary and secondary regimes), the analogy solution does yield

an approximately constant value of Nusselt number, justifying the assumption of a uniform Nusselt number in the primary regime. Thus, the predicted heat-transfer characteristics of the primary regime are in accord with those found by previous workers [7, 9, 10, 11].

The analogy solution demonstrates the stabilising effect of an axial flow, and, after criticality, the constant rise in Nusselt number with Taylor number. Also, it can be seen that for a given value of Taylor number, the prevailing Nusselt number decreases with increasing axial Reynolds number, emphasising the damping effect of the imposed axial flow on the internal motions of the vortices.

Figures 1(a) and (b) also indicate that there is little difference between the Nusselt numbers obtaining under given conditions of Taylor and axial Reynolds numbers for both radius ratios ($N = 0.955$ and 0.8), although those for $N = 0.8$ are always slightly lower than those for $N = 0.955$. Thus, this solution implies that, under given conditions, the prevailing Nusselt is virtually independent of radius ratio.

COMPARISON OF NUSSELT NUMBERS OBTAINED BY EXPERIMENT AND BY THE REYNOLDS ANALOGY SOLUTION

The apparatus used for the determination of the experimental Nusselt numbers is described in [3] and is shown diagrammatically in Fig. 2. In essence, it consisted of a vertical concentric annulus, through which the working fluid, air, was passed. It was comprised of a stationary steel tube of I.D. 139.7 mm and an inner rotatable cylinder of Tufnol, a good thermal insulator chosen to ensure adiabatic conditions. Two such cylinders existed of diameters 133.4 mm and 111.8 mm, giving radius ratios of 0.955 and 0.8 respectively; the length of these cylinders was 1.82 m.

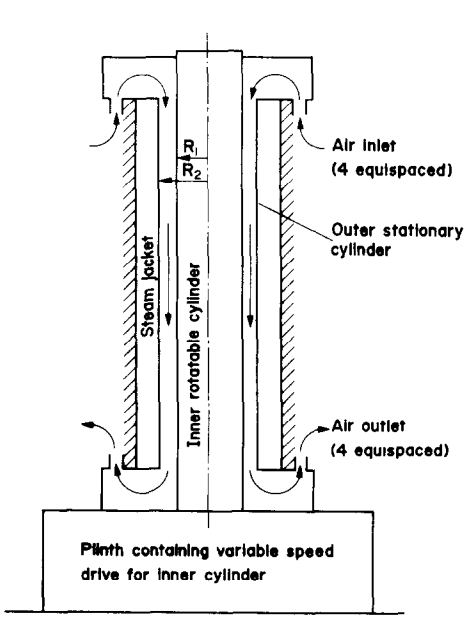

FIG. 2. Diagram of apparatus.

The stationary steel tube was heated by condensing wet steam and so the outer surface of the annulus was isothermal while the inner surface should have been adiabatic. However, it was found during the course of the experiments that heat was transferred to a small extent through the inner cylinder and so the latter condition was not fulfilled.

To permit the measurement of velocity and temperature profiles as the flow developed through the annular gap, 29 measuring stations were provided. These stations were arranged in four vertical lines at 90° intervals along the length of the gap. Three of the lines had seven stations while a fourth had eight. The stations were not equispaced but were concentrated at each end of the annular gap to permit study of the entrance region.

To obtain the value of average axial velocity in the annular gap necessary for the evaluation of the axial Reynolds number, velocity profiles were obtained across the gap, a reading being taken at every one-tenth of the gap. DISA hot wire anemometry equipment was used for this determination. Radial temperature profiles across the annulus were also obtained. Since a suitable thermocouple probe was not commercially available for the measurement of temperatures in the gap, it was necessary to develop a special fine wire probe. The output of this probe was monitored by a Solartron data-logger system. The wall temperature, T_w, was determined by positioning the probe flush to the outer wall. While it was recognised that small errors in this value could markedly affect the calculated values of the Nusselt number, the possibility of such errors was minimised by the use of a single probe to acquire all the temperatures across the gap. Accuracy was also aided by the good temperature resolution of the probe, viz 0.0625°C.

Although the temperature gradients were estimated by visual means from graphs of temperature against radial distance, it should be noted that in the 20% of the gap nearest to the outer stationary wall, nine equispaced readings were taken. Thereafter, readings were taken at every 10% of the gap.

Figure 3 is a typical carpet plot of radial temperature profiles for $N = N = 0.955$, $Re_a = 1200$ and five values of Ta. It should be noted, however, that these particular profiles were not used as a source of values for Fig. 4(c).

From the temperature gradients at the outer stationary wall, local values of the Nusselt number were calculated thus:

$$Nu = \frac{2d(\partial T/\partial R)}{T_w - T_{av}}. \tag{37}$$

The Nusselt numbers are presented in Figs 4 and 5, for three values of axial Reynolds number, $Re_a = 400$, 800 and 1200, and for two values of radius ratio, $N = 0.955$ and 0.8. These figures show the variation of local Nusselt number with Taylor number, plotted on logarithmic axes, for a given value of axial Reynolds number. Superimposed on

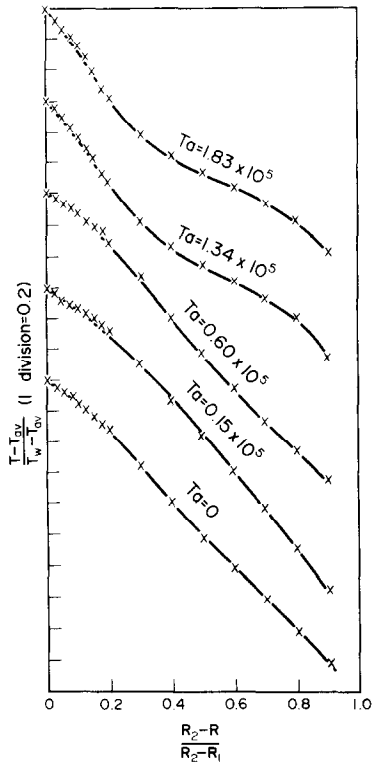

FIG. 3. Radial temperature profiles, $N = 0.955$, $Re_a = 1200$.

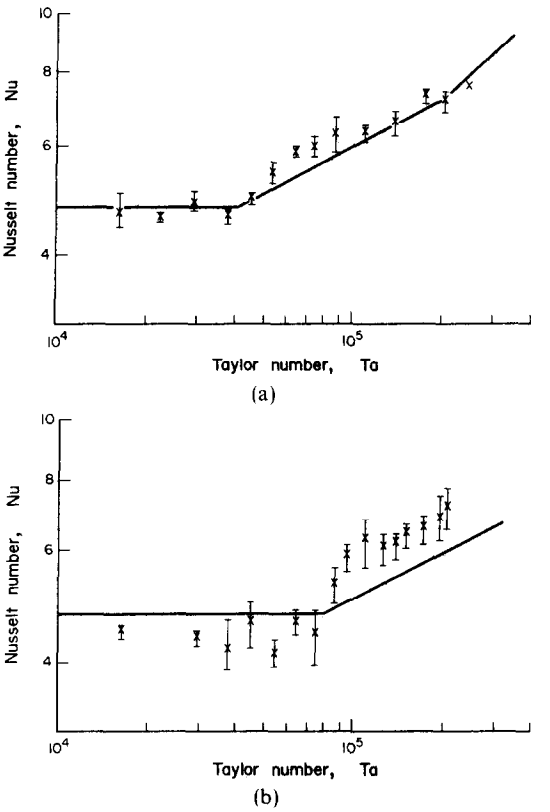

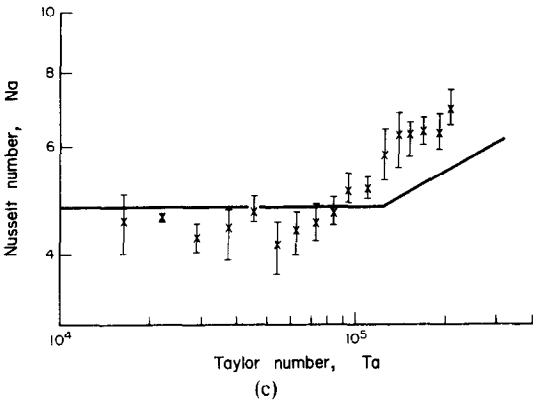

FIG. 4.
(a) Nusselt number vs Taylor number, $N = 0.955$, $Re_a = 400$.
(b) Nusselt number vs Taylor number, $N = 0.955$, $Re_a = 800$.
(c) Nusselt number vs Taylor number, $N = 0.955$, $Re_a = 1200$.

these figures are the lines which represent the results of the Reynolds analogy solution. For each Taylor number, between two and four tests were performed. In the figures, the range of the local Nusselt number obtained in these tests is shown with the mean value marked within that range.

The general trends of the results of Figs. 4 and 5 are seen to be in accord with those of previous investigations [9–11], in that the Nusselt number remains approximately constant in the primary regime, whilst in the secondary regime, the Nusselt number rises steadily with Taylor number. The demarcation between the two regimes is sharp, and the stabilising effect of the imposed axial flow is apparent.

A detailed consideration of the results for $N = 0.955$ (Fig. 4) indicates that in the primary regime, although a considerable amount of scatter is apparent, the Nusselt number bears no relationship to the prevailing Taylor number, and can consequently be considered as a constant value. This constant value is less than that predicted by the analogy solution and by El-Shaarawi [7], which can be attributed to the effects of heat transfer at the rotor surface, causing a decrease in the average temperature across the gap, which results in a lower value of Nusselt number.

Considering Fig. 4(a), the critical Taylor number and the slope of the graph in the secondary regime, as found by experiment and theory, are seen to be in agreement. Unfortunately, the restricted Taylor number range allowed by this radius ratio only gave experimental results up to the predicted onset of the tertiary regime, and thus the existence of this regime could not be verified from these results.

For $Re_a = 800$ and 1200, the agreement is less good [Figs. 4(b) and (c)]. The experimentally determined value of critical Taylor number is slightly less than that obtained from the analogy and consequently the Nusselt numbers obtaining in the secondary regime are higher than predicted. The slope of the secondary regime is, however, similar for both cases. It should be noted that the limited Taylor number range of this radius ratio only allows the

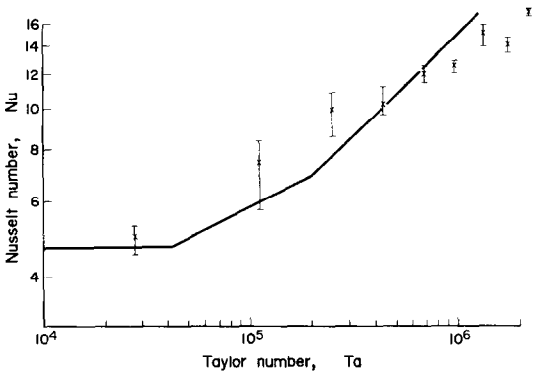

(a)

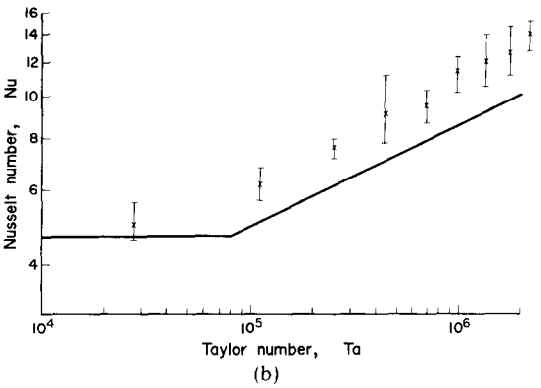

(b)

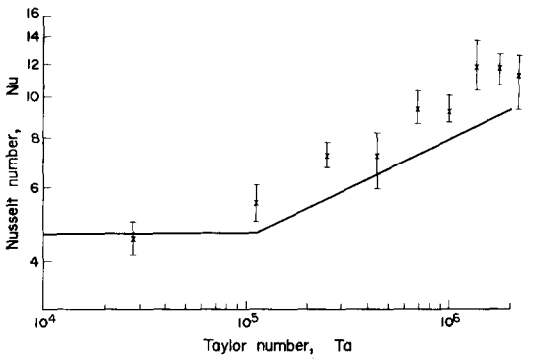

(c)

FIG. 5.
(a) Nusselt number vs Taylor number, $N = 0.8$, $Re_a = 400$.
(b) Nusselt number vs Taylor number, $N = 0.8$, $Re_a = 800$.
(c) Nusselt number vs Taylor number, $N = 0.8$, $Re_a = 1200$.

acquisition of results up to a maximum Taylor number of 200 000, which are to be compared with an analogy solution applicable over the range, $Ta_c \leqslant Ta \leqslant 2 \times 10^6$. Consequently, small errors in the determination of the critical Taylor number from the shear stress study of [3], which are subsequently included in the analogy solution, can easily result in the observed differences, when viewed over such a limited range. The values of critical Taylor number (Table 1) were assessed from the shear stress results taken on a rig of radius ratio $N = 0.833$, and were assumed to apply to the larger radius ratio, $N = 0.955$. However, in justification of this assumption, the critical values obtained by Coney [11], when studying experimentally heat transfer through the outer stationary wall of an annulus of $N = 0.897$, are in close agreement with those of the present study, the mean difference between the two sets of results being 6.6% for $300 \leqslant Re_a \leqslant 1600$. A graph of these results appears in [8].

The results for $N = 0.8$ (Fig. 5) show that the experimental measurements are generally confined to the secondary regime of flow, owing to the high values of Taylor number prevailing even at low rotational speed. Consequently, no conclusions can be drawn regarding criticality under such conditions. The spread of the data points in these figures is generally worse than was encountered for the case of $N = 0.955$ (Fig. 4), and this can be attributed to two effects. Firstly, the temperature probe, when positioned in the central portion of the gap, indicated that temperature fluctuations were occurring as the vortices drifted past the sensor. This observation accords with Hoh *et al.* [12], who considered the axial variation of temperature along an annulus, subjected to Taylor vortex flow, but without axial flow, which exhibited a small sinusoidal disturbance in the axial temperature field. The larger, more vigorous vortices associated with the radius ratio of $N = 0.8$ caused greater fluctuations in temperature than for the case of $N = 0.955$, and result in less accurate radial temperature profiles and Nusselt numbers. Secondly, occasionally the radial temperature profiles obtained from two traverses performed under identical conditions, but a short time apart, exhibited a marked change in shape, suggesting that the vortices had undergone a fundamental change. However, this effect occurred so infrequently that the postulated change in form could not be checked.

For $Re_a = 400$, [Fig. 5(a)] the experimental results are higher than those predicted theoretically in the secondary regime. However, the data points exhibit a slope, up to the maximum Taylor number of 2×10^6, similar to that of the analogy solution in the secondary regime. Thus the existence of the postulated tertiary regime is not confirmed by these experimental results.

The results for $Re_a = 800$ and 1200 [Figs 5(b) and (c)] also indicate that the theoretical values of Nusselt number are generally lower than those found experimentally, and that use of the analogy solution could lead, in the worst case, to an underestimate of approximately 40% in the value of the prevailing Nusselt number.

Thus, for the case of $N = 0.955$, the analogy solution adequately predicted the Nusselt numbers obtaining in combined axial and Taylor vortex flows, allowing for the small differences induced by the use of a critical Taylor number applicable to a radius ratio of $N = 0.833$, discussed earlier. Although the agreement for the case of $N = 0.8$ was encouraging, it is considered that the analogy is only truly applicable to the narrow gap case.

The fact that the experimental results are essentially parallel to those of the "narrow gap" analogy, in the secondary regime, for both $N = 0.955$ and 0.8, lends some support to the mechanisms and flow regions postulated in the analogy. Thus, it is suggested that, accepting the imperfect representation of the flow conditions obtaining in the wide gap case, the narrow gap analogy solution can be used to predict the Nusselt numbers prevailing under wide gap conditions. To achieve closer agreement between the predicted and experimental results for $N = 0.8$, an empirical factor should be introduced into the analogy solution. Whilst such an approach cannot be justified physically, it does allow the use of a simpler equation than would be derived from a 'wide gap' analogy solution.

Acknowledgement—By permission of the Council of the Institution of Mechanical Engineers, Figs. 2 and 6 are reprinted from "The effect of Taylor vortex flow on the development length in concentric annuli" by Simmers and Coney, and Table 1 is reprinted from [8].

REFERENCES

1. I. S. Bjorklund and W. M. Kays, Heat transfer between rotating concentric cylinders, *J. Heat Transfer* **81**, 175–186 (1959).
2. S. I. Pai, Turbulent flow between rotating cylinders, *NACA, Tech. Note No.* 892, (1943).
3. D. A. Simmers, The development, hydrodynamics and heat transfer characteristics of a rotary heat exchanger, Ph. D. Thesis, Leeds University, England. (1976).
4. G. I. Taylor, Distribution of velocity and temperature between concentric rotating cylinders, *Proc. R. Soc. Ser. A* **151**, 494–512 (1935).
5. J. R. Flower and N. Macleod, The radial transfer of mass and momentum in an axial fluid stream between co-axial rotating cylinders, II—The analogy between mass and momentum transfer in streams containing secondary flows, *Chem. Engng Sci.* **24**, 615–622 (1969).
6. R. J. Donnelly and N. J. Simon, An empirical torque relation for supercritical flow between rotating cylinders, *J. Fluid Mech.* **7**, 401–418 (1960). Also Appendix by G. K. Batchelor, A theoretical model of the flow at speeds far above the critical.
7. M. A. I. El-Shaarawi, Heat transfer and hydrodynamics in the entrance region of concentric annuli with stationary and rotating inner walls, Ph.D. Thesis, Department of Mechanical Engineering, The University of Leeds, Leeds, England. (July 1974.)
8. J. E. R. Coney and D. A. Simmers, A study of fully-developed laminar axial flow and Taylor vortex flow by means of shear stress measurements, *J. Mech. Engng Sci. (Inst. Mech. Engng)* **20**, 6 (1978).
9. K. M. Becker and J. Kaye, Measurements of diabatic flow in an annulus with an inner rotating cylinder, *J. Heat Transfer* **84**, 97–105 (1962).
10. C. Gazley, Heat transfer characteristics of the rotational and axial flow between concentric cylinders, *Trans. Am. Soc. Mech. Engrs* **80**, 79–90 (1958).
11. J. E. R. Coney, Taylor vortex flow with special reference to rotary heat exchangers, Ph.D. Thesis, Department of Mechanical Engineering, University of Leeds, Leeds, England. (September 1971.)
12. C. Y. Hoh, J. L. Nardacci and A. H. Nissan, Heat transfer characteristics of fluids moving in a Taylor system of vortices, *A.I.Ch.E. Jl* **10**, 194–202 (1964).

SOLUTION SELON L'ANALOGIE DE REYNOLDS DU TRANSFERT THERMIQUE POUR DES ECOULEMENTS COMBINES AXIAUX ET A TOURBILLONS DE TAYLOR

Résumé—On développe une solution, semblable à celle de l'analogie de Reynolds entre chaleur et quantité de mouvement, pour le transfert thermique entre la surface externe d'une espace annulaire formé par un cylindre externe fixe et un cylindre interne tournant avec un fluide entre eux; il existe dans le fluide des tourbillons de Taylor et un écoulement axial imposé.

Pour simplifier la solution, on suppose un profil de vitesse en trois parties avec une sous-couche laminaire adjacente à la surface externe, une couche intermédiaire et un noyau à vitesse constante dans la partie centrale de l'anneau fluide.

On obtient des expressions pour les épaisseurs et les chutes de température dans la sous-couche laminaire et la couche intermédiaire. Ceci conduit aux nombres de Nusselt qui sont comparés avec ceux obtenus expérimentalement.

EINE LÖSUNG MITTELS DER REYNOLDS-ANALOGIE FÜR DAS WÄRMEÜBERGANGSVERHALTEN EINER KOMBINIERTEN AXIAL—UND TAYLOR-WIRBEL-STRÖMUNG

Zusammenfassung—Eine Lösung ähnlich der Reynolds-Analogie für Wärme- und Impulstransport wurde für den Wärmeübergang an der äußeren Fläche eines ringförmigen Spalts entwickelt, der aus einem ruhenden Außenzylinder und einem rotierenden Innenzylinder besteht Im Fluid existieren Taylor-wirbel mit überlagerter axialer Strömung. Zur Vereinfachung der Lösung wurde ein Geschwindigkeitsprofil angenommen, das aus drei Abschnitten besteht, nämlich aus einer laminaren Unterschicht an der Außenfläche des Ringspalts, einer Pufferschicht und einer Kernzone mit konstanter Geschwindigkeit im Zentrum des ringförmigen Spalts. Ausdrücke für die Stärke und den Temperaturabfall in der laminaren und in der Pufferschicht wurden formuliert. Diese wurden benutzt, um Nusselt-Zahlen zu bestimmen, die dann mit experimentell ermittelten verglichen wurden.

ИСПОЛЬЗОВАНИЕ АНАЛОГИЙ РЕЙНОЛЬДСА ДЛЯ ОПРЕДЕЛЕНИЯ ХАРАКТЕРИСТИК ТЕПЛООБМЕНА СОВМЕСТНЫХ ТЭЙЛЕРОВСКИХ ВИХРЕВЫХ И АКСИАЛЬНЫХ ПОТОКОВ

Аннотация — С помощью аналогии Рейнольдса получено решение задачи о переносе тепла между внешней поверхностью кольцевого канала, образованного неподвижным внешним цилиндром и вращающимся внутренним цилиндром, и жидкостью в зазоре между ними при условии наложения на аксиальное течение Тэйлоровских вихрей. Для упрощения анализа принято, что профиль скорости состоит из ламинарного подслоя, прилегающего к внешней поверхности зазора, переходного слоя и области ядра с постоянной скоростью, находящейся в центральной части кольцевого зазора. Получены выражения для определения толщины ламинарного подслоя и переходного слоя, а также перепадов температур в их поперечных сечениях. С помощью этих соотношений рассчитаны значения числа Нуссельта, которые затем были сопоставлены с экспериментальными данными.